Journal of Physics: Conference Series

PAPER • **OPEN ACCESS**

The fabrication of zinc oxide nanorods and nanowires by solgel immersion methods

To cite this article: A A Ameer *et al* 2019 *J. Phys.: Conf. Ser.* **1170** 012005

IOP Conf. Series: Journal of Physics: Conf. Series **1170** (2019) 012005 doi:10.1088/1742-6596/1170/1/012005

The fabrication of zinc oxide nanorods and nanowires by sol-gel immersion methods

A A Ameer[1,2], A B Suriani[1,2*], A R Jabur[3], N Hashim[1], Fatiatun[1,2] and K Zaid[1,2]

[1] Nanotechnology Research Centre, Faculty of Science and Mathematics, Universiti Pendidikan Sultan Idris, 35900 Tanjung Malim, Perak, Malaysia
[2] Department of Physics, Faculty of Science and Mathematics, Universiti Pendidikan Sultan Idris, 35900 Tanjung Malim, Perak, Malaysia
[3] Department of Materials Engineering, University of Technology, Baghdad, Iraq

*Corresponding author: absuriani@yahoo.com

Abstract. The zinc oxide (ZnO) nanorods (NRs) (4 hours) and nanowires (NWs) (12 and 24 hours) were synthesized on the magnesium ZnO (MgZnO) seed layer by using sol-gel immersion method. The ZnO NRs and NWs were characterized by FESEM, XRD, UV-Vis and four-point probe measurement. The FESEM images showed uniform, dense and vertically aligned structure. The smallest diameter observed in ZnO NWs (24 hours) in the range ~ 47.6-99.2 nm. The XRD spectra also presented the *c*-axis growth of ZnO NRs and NWs. The ZnO NWs (24 hours) demonstrated higher transmittance and electrical conductivity of ~77.8% and 2.6×10^{-1} S cm^{-1} as compared to ZnO NRs of 66.7% and 1.1×10^{-2} S cm^{-1}, respectively. Therefore, the ZnO NWs (24 hours) showed a good structure to be applied in solar cells and UV sensor applications.

1. Introduction

In the last few years, the one dimensional (1D) nanostructures of zinc oxide (ZnO) [1] got an intensive attention due to its wide band gap energy (~3.37 eV) and high binding exciton energy (~60 meV) [2]. The ZnO has many morphology structures such as nanorods (NRs) [3], nanosheets [4], nanorings [5], nanowires (NWs) [6], nanoflowers (NFs) [7] and nanostars [8]. Among all, the ZnO NRs and NWs are usual utilized morphology in many applications due to higher surface area as compared to another nanostructures [9]. The ZnO NRs and NWs can be synthesized by using chemical vapour deposition (CVD) [10], pulse laser deposition (PLD) [11], vapour liquid solid (VLS) [12], metal organic chemical vapour deposition (MOCVD) [13], arc discharge [14], hydrothermal [15] and sol-gel immersion method [16].However, the sol-gel immersion method was commonly used to synthesize the ZnO NRs and NWs due to its green, inexpensive and low temperature [17].

The ZnO nanostructures are commonly grown on the seed layer such as aurum (Au), silicon dioxide (SiO_2) [18], magnesium oxide (MgO) [19], magnesium ZnO (MgZnO) [20] and aluminum zinc oxide (AlZnO) [21]. Among all, the MgZnO was chosen as seed layer due to its high similarity in the ionic radii which the ionic radii of Mg and ZnO were ~ 0.72 and ~ 0.74Å, respectively. The seed layer is needed for the ZnO growth because it can decrease the thermodynamic barrier [21-22]. The ZnO nanostructures without seed layer presented lower quality [24] than ZnO with seed layer. The MgZnO seed layer can be fabricated by using dip coating [25], magnetron sputtering technique [26] and spin coating [26-27]. The spin coating method was preferred to fabricate the MgZnO seed layer because of its low cost, simple preparation and easy to produce a uniform thin film [29]. The MgZnO was fabricated on the glass substrate.

The ZnO has been widely developed in many application such as gas sensor [30], vibration sensor [31], UV sensor [32], solar cell [17] and power energy storage [33]. Among all, the UV sensor application got an intensive attention due to large scale applications such as optical communication, flame detection and missile launching detection [34]. In this paper, the structural, optical and electrical properties of ZnO NRs and NWs were characterized by using field emission scanning microscopy (FESEM), X-ray diffraction (XRD), ultraviolet visible (UV-Vis) and four-point probe measurement.

2. Materials and Methods

Prior the fabrication of MgZnO seed layer, the glass substrates (2 x 2) cm^2 were cleaned by using acetone and DI water for 10 and 5 minutes, respectively. The MgZnO seed layer solution was prepared by mixing 0.4 M of zinc acetate dehydrate ($Zn(CH_3COO)_2.2H_2O$) and magnesium nitrate hexahydrate ($Mg(NO_3)_2.6H_2O$), 10 ml of 2-methoxyethanol ($C_3H_8O_2$) as a solvent and 0.25 ml of mono-ethanolamine (C_2H_7NO) as a stabilizer. The prepared solution was sonicated at 50 °C for 30 minutes followed by stirring the solution for 2 hours at room temperature in order to get a homogeneous solution. Afterward, the MgZnO solution was deposited (10 drop) on the glass substrate using a spin-coater for 1 minute at 3000 rpm. The samples were then annealed in oven at 150 °C for 10 minutes. These processes were repeated for 5 times followed by post annealing process for 1 hour at 500 °C.

The ZnO NRs and NWs were then grown on the MgZnO seed layer by using sol-gel immersion method. The ZnO solution was prepared by mixing 0.05 and 0.025 M of zinc nitrate hexahydrate [$Zn(NO_3)_3.6H_2O$] and hexamethylenetetramine ($C_6H_{12}N_4$, HMT), respectively in 200 ml of DI water. The ZnO solution was then sonicated at 50 °C for 30 minutes and stirred for 2 hours at room temperature followed ageing process for 24 hours at room temperature in order to get a homogenous solution. Afterward, the prepared MgZnO seed layer was immersed in the ZnO solution in water bath for 4 hours at 95 °C, 12 and 24 hours at 90 °C in order to synthesize of ZnO NRs and NWs, respectively. The synthesized ZnO samples (ZnO NRs (4 hours), ZnO NWs (12 and 24) hours) were then taken out and rinsed in DI water. The ZnO samples were dried in oven for 10 minutes at 150 °C and post annealed for 1 hour at 500 °C in a furnace.

3. Result and Discussion

Fig. 1 present the FESEM images of ZnO NRs and NWs synthesized by sol-gel immersion method. The MgZnO seed layer (Fig. 1 (a)) shows a dense and uniform film with the diameter and thickness of 13-32 nm and 0.5-1 µm, respectively. However, a white agglomerations can be also observed in this figure which was believed due to inhomogeneous MgZnO solutions. Fig. 1 (b) and (d) show the top view of ZnO NWs (24 hours) and ZnO NWs (12 hours) with the hexagonal shaped diameter of ~ 47.6-99.2 and 65.4-115 nm, respectively. This presents that the ZnO NWs (24 hours) shows lower diameter as compared to the ZnO NWs (12 hours) due to its lower pH ratio in the ZnO solutions. This indicates higher surface area of ZnO NWs (24 hours) than ZnO NWs (12 hours) [35].

In the other side, the increasing synthesis time of ZnO NWs from 12 to 24 hours demonstrates the increment of density. The side view of ZnO NWs (24 hours) (Fig 1. (c)) and ZnO NWs (12 hours) (Fig. 1 (e)) show the thickness of around 2-2.20 and 2.1-2.6 µm, respectively. Lower thickness of ZnO NWs (24 hours) than ZnO NWs (12 hours) was also believed due to decreasing of pH ratio of ZnO solutions during the ZnO growth. Fig 1 (f)-(g) presents the top and side view of ZnO NRs with the diameter and thickness of 80-120 nm and 1.4-1.7 µm, respectively. This ZnO NRs (4 hours) also shows the hexagonal shaped (red arrow). This hexagonal shaped was produced by HMT in the ZnO solution during the ZnO growth [36]. The ZnO NFs are also observed on the ZnO NWs (24 hours) (Fig. 1 (h)) and ZnO NRs (4 hours) (Fig. 1 (i)), respectively. The formation of ZnO NF was believed due to high OH^- ions concentration and exceed the critical value of ZnO solution thus affected to the ZnO nanostructure [37]. The increasing synthesis time of ZnO NWs from 12 to 24 hours presents the decrement of produced ZnO NFs.

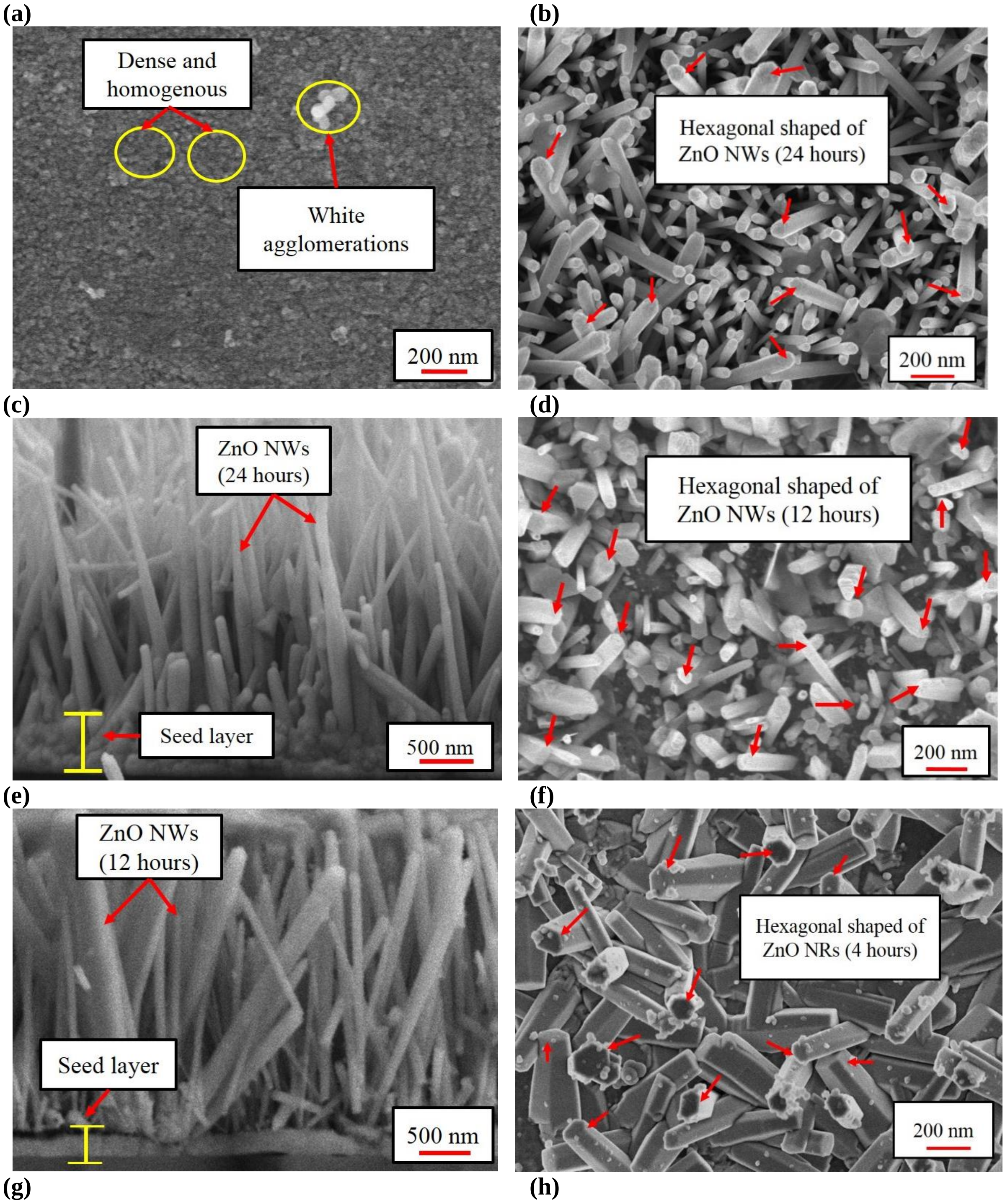
(a)
Dense and homogenous
White agglomerations
200 nm
(b)
Hexagonal shaped of ZnO NWs (24 hours)
200 nm
(c)
ZnO NWs (24 hours)
Seed layer
500 nm
(d)
Hexagonal shaped of ZnO NWs (12 hours)
200 nm
(e)
ZnO NWs (12 hours)
Seed layer
500 nm
(f)
Hexagonal shaped of ZnO NRs (4 hours)
200 nm
(g)
(h)

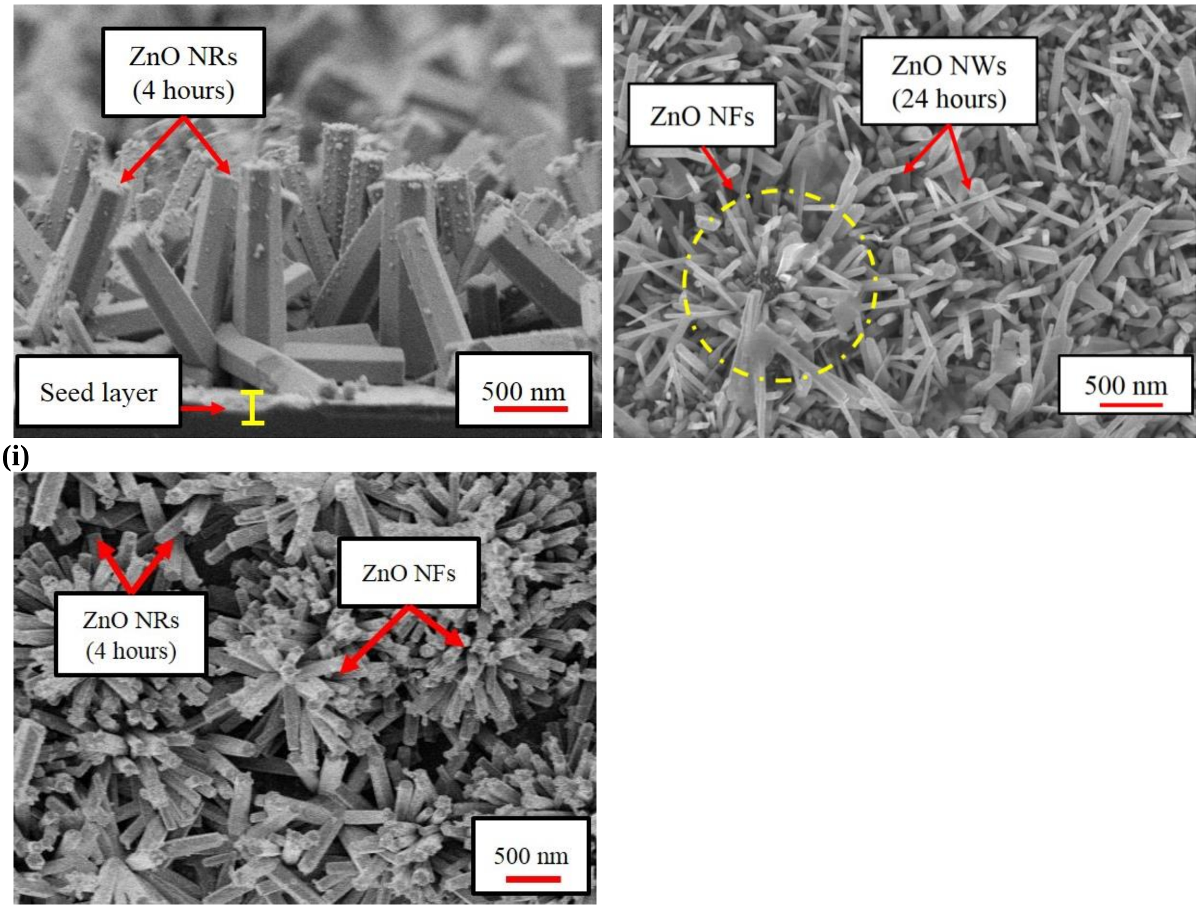

Figure 1. FESEM images of (a) MgZnO seed layer, (b) top view of ZnO NWs (24 hours), (c) cross section of ZnO NWs (24 hours), (d) top view of ZnO NWs (12 hours), (e) cross section of ZnO NWs (12 hours), (f) top view of ZnO NRs (4 hours), (g) cross section of ZnO NRs (4 hours) (h) top view of ZnO NFs on top of ZnO NWs (24 hours), (i) top view of ZnO NFs on top of ZnO NRs (4 hours).

The structural properties of ZnO NRs and NWs can be determined by using XRD spectra in Fig. 2. The ZnO NWs and NRs show hexagonal wurtzite structure and present 10 diffraction peaks which are 100, 002, 101, 102, 110, 103, 112, 201, 004 and 202 peaks. These peaks confirm that the ZnO NWs and NRs have hexagonal wurtzite structure as reported by PDF 01-078-4603. The (002) peak at 34.8° demonstrates the highest and sharpness peak in the XRD spectra of ZnO NWs and NRs. This reveals the ZnO growth along c-axis with a good crystallinity [38]. The other peaks present low intensity which was believed due to imperfections and increasing the grain boundary of ZnO NWs and NRs. The ZnO NWs (24 hours) demonstrates higher peak intensity as compared to the ZnO NWs (12 hours). This indicates high crystallinity of ZnO NWs (24 hours). The ZnO NWs (24 hours) also presents lower crystallite size of ~ 30 nm than ZnO NWs (12 hours) of ~ 32.5 nm. The ZnO NRs shows high crystallite size of ~ 39 nm.

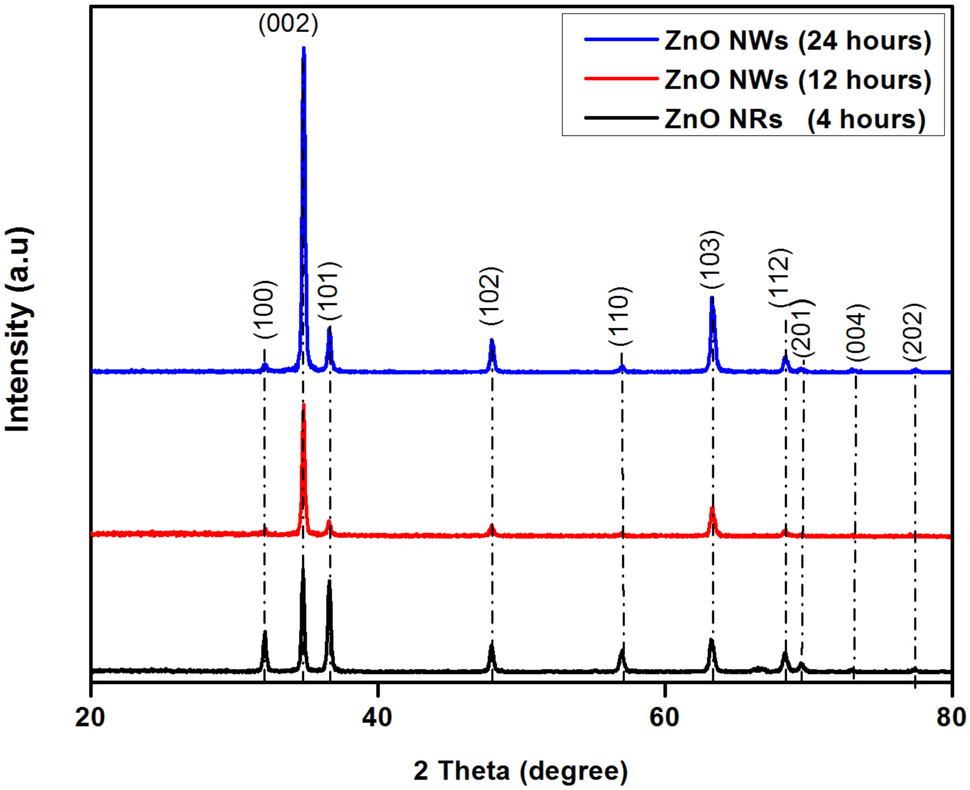

Figure 2. XRD pattern of ZnO NRs (4 hours) and ZnO NWs (12 and 24) hours

The transmittance spectra of ZnO NRs (4 hours) and ZnO NWs (12 and 24) hours are presented in (Figure 3) which can be determined the optical properties of ZnO. All the samples included in a high transmittance due to its value over 66% in the visible range. However, the highest transmittance was observed in the ZnO NWs (24 hours) of ~77.8%. This indicates that the ZnO NWs (24 hours) shows higher transmittance than ZnO NWs (12 hours) of ~74.1%. This was believed due to lower diameter of ZnO NWs (24 hours) (see Figure 1 (f)) than ZnO NWs (12 hours). For the ZnO NRs (4 hours), it demonstrates low transmittance of approximately ~66.7%. Therefore, the ZnO NWs shows better optical properties as compared to the ZnO NRs and indicates suitable to be applied for UV-sensor and solar cell application.

Figure 4 shows the I-V curves of ZnO NRs (4 hours) and ZnO NWs (12 and 24) hours. Based on the I-V curves, the ZnO NWs (24 hours) presents higher conductivity of ~2.6×10^{-1} S cm^{-1} than ZnO NWs (12 hours) of ~1.6×10^{-1} S cm^{-1}. This was believed due to higher surface area [39] of ZnO NWs (24 hours) than ZnO NWs (12 hours). High surface area of ZnO NWs (24 hours) leads to increase the electron movement thus suitable to be applied for UV sensor and solar cell application. The ZnO NRs (4 hours) demonstrates low conductivity of ~1.1×10^{-2} S cm^{-1} due to its low surface area.

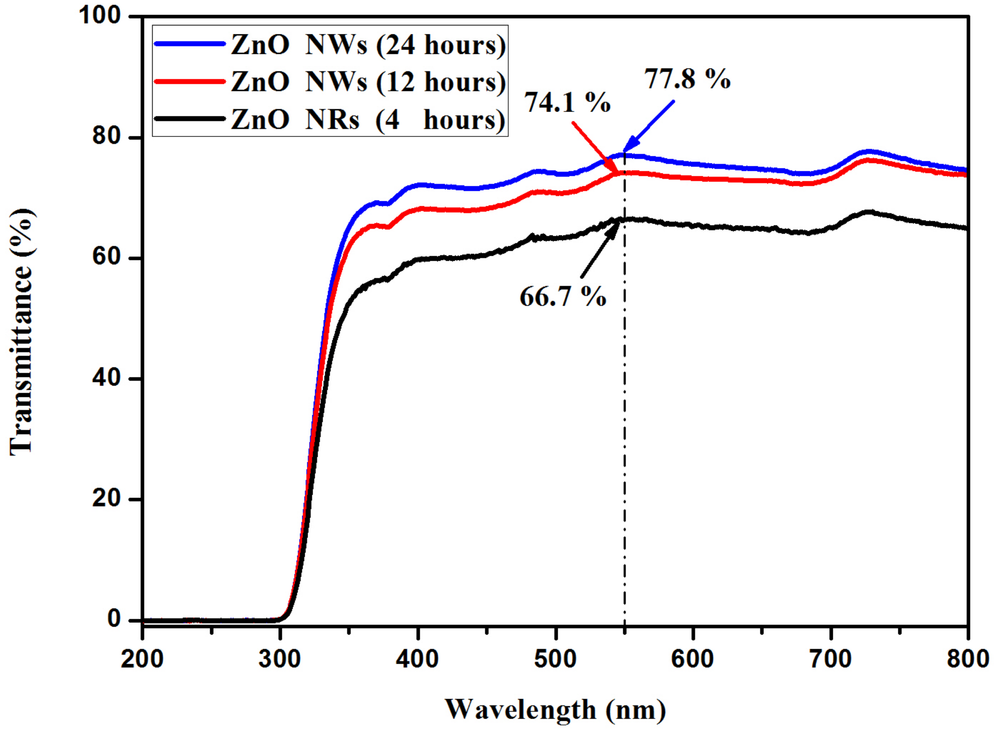

Figure 3. Transmittance spectra of ZnO NRs (4 hours) and ZnO NWs (12 and 24) hours

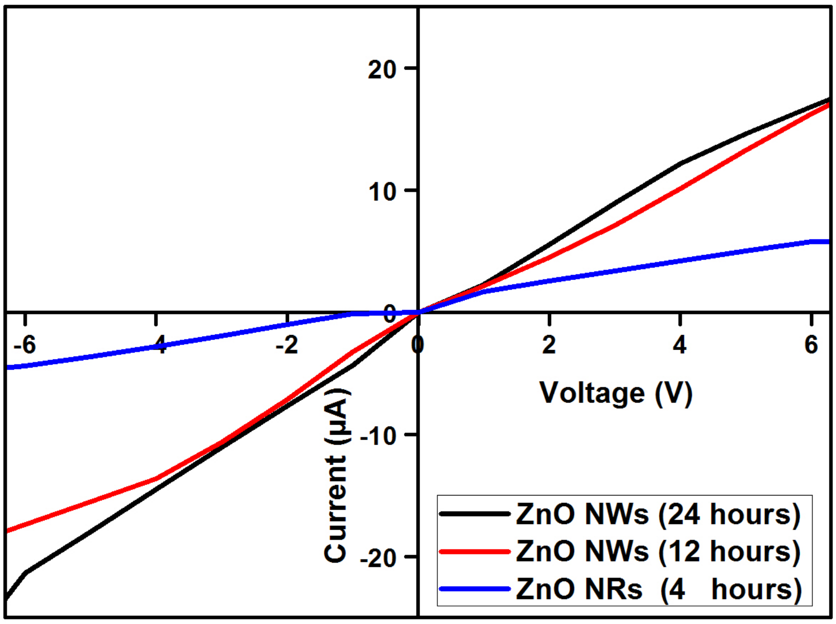

Figure 4. I-V curves of ZnO NRs (4 hours) and ZnO NWs (12 and 24) hours

4. Conclusion

The ZnO NRs (4 hours) and ZnO NWs (12 and 24) hours were successfully synthesized by sol-gel immersion method on the MgZnO seed layer. The structural properties of ZnO NRs and NWs were investigated by FESEM and XRD analysis. The FESEM images show that the ZnO NWs (24 hours) presents smaller diameter of ~47.6–99.2 nm than ZnO NWs (12 hours) due to its higher surface area. The XRD analysis also demonstrates that the ZnO NWs (24 hours) shows higher crystallinity than ZnO NWs (12 hours). Based on the transmittance spectra, the ZnO NWs (24 hours) also shows the higher transmittance of 77.8% than ZnO NWs (12 hours) of 74.1%. The I-V measurement also presents that the ZnO NWs (24 hours) shows higher conductivity of ~2.6×10^{-1} S cm^{-1} than ZnO NWs (12 hours) of ~1.6×10^{-1} S cm^{-1}. Therefore, the ZnO NWs (24 hours) reveals better structural, optical and electrical properties as compared to ZnO NWs (12 hours) and ZnO NRs (4 hours) which also indicates suitable to be applied for UV-sensor and solar cell applications.

Acknowledgement

The authors would like to express their appreciation to the National Nanotechnology Directorate Division (2014-0015-102-03) and Fundamental Research Grant Scheme (Grant Code: 2015-0154-102-02) for their financial support.

References

[1] Vabbina P K, Kaushik A, Pokhrel N, Bhansali S and Pala N 2015 *J Biosens Bioelectron* **63** 124
[2] Marin O, Tirado M, Budini N, Mosquera E and Figueroa C 2016 *J Mater Sci Semicond Process* **56** 59
[3] Yang, Qin, Cai H, Hu Z, Duan Z, Li Y, Sun J, Xu N and Wu J 2014 *J Mater Res Express* **1** 015010
[4] Zhang, Bin, Wang F, Zhu C, Li Q, Song J, Zheng M, Ma L and Shen W 2016 *J Nano-Micro Lett* **8** 137
[5] Yousefi R 2015 *J Cryst Eng Comm* **17** 2698
[6] Gu Y Z, Lu H L, Zhang Y, Wang P F, Ding S J and Zhang D W 2015 *J Opt Express* **23** 24456
[7] Wu X, Chen H, Gong L, Qu F and Zheng Y 2011 *J Adv Nat Sci Nanosci Nanotechnol* **2** 3
[8] Kwong T L and Yung K F 2016 *J Renew Energy* **90** 450
[9] Hung C M, Le D T T and Van Hieu N 2017 *J Sci Adv Mater Devices* **2** 263
[10] Wu J, J-J. and Liu S C 2002 *J Adv Mater* **14** 215
[11] Sun Y, Fuge G M and Ashfold M N R 2004 *J Chem Phys Lett* **396** 21
[12] Zhao Q X, Klason P and Willander M 2007 *J Appl Phys A.* **88** 27
[13] Lee W, Jeong M and Myoung J 2004 *J Acta Mater* **52** 3949
[14] Fang F, Kennedy J, Carder D A, Futter J, Murmu P and Markwitz A 2010 *J Nanosci Nanotechnol* **10** 8239
[15] Guo M, Diao P and Cai S 2005 *J. Solid State Chem* **178** 1864
[16] Foo K L, Hashim U, Muhammad K and Voon C H 2014 *J Nanoscale Res Lett* **9** 1
[17] Suriani A B, Mohamed A, Hashim N, Rosmi M S, Mamat M H, Malek M F, Salifairus M J and Khalil H P S A 2018 *J. Optik.* **161** 70
[18] Xu C H, You Y F, Wang J Z, Ge S F, Fong W K, Leung K and Surya C 2013 *J Superlattices Microstruct* **61** 97
[19] Kong, Jieying, Li L, Yang Z and Liu J 2014 *J Vac Sci Technol B Nanotechnol Microelectron: Mater Process Meas Phenom* **10** 1
[20] Suriani A B, Safitri R N, Mohamed A, Alfarisa S, Isa I M, Kamari A, Hashim N, Ahmad M K, Malek M F and Rusop M 2015 *J Mater Lett* **149** 66
[21] Kim K H, Utashiro K, Abe Y and Kawamura M 2014 *J Mater* **7** 2522
[22] Park, Won Il and Yi G C 2004 *J Adv Mater* **16** 87
[23] Amin, Gul, Asif M H, Zainelabdin A, Zaman S, Nur O and Willander M 2011 *J Nanomater* **5** 2011
[24] Dong, Jing-Jing, Chun-Yang Zhen, Hui-Ying Hao, Jie Xing, Zi-Li Zhang, Zhi-Yuan Zheng and Xing-Wang Zhang 2013 *J Nanoscale Res Lett* **8** 378
[25] Malek M F, Mamat M H, Sahdan M Z, Zahidi M M, Khusaimi Z and Mahmood M R 2013 *J Thin Solid Films* **527** 102

[26] Zhou H, Fang G, Liu N and Zhao X 2011 *J. Nanoscale Res Lett* **6** 1
[27] Malek M F, Mamat M H, Sahdan M Z, Zahidi M M, Khusaimi Z and Mahmood M R 2013 *J Thin Solid Films* **527** 102
[28] Suriani A B, Safitri R N, Mohamed A, Alfarisa S, Isa I M, Kamari A, Hashim N, Ahmad M K, Malek M F and Rusop M 2015 *J Mater Lett* **149** 66
[29] Suriani A B, Alfarisa S, Mohamed A, Kamari A, Hashim N, Isa I M, Mamat M H, Malek M F and Ahmad M K 2015 *J Alloys Compd* **642** 111
[30] Li Y, Gong J, He G and Deng Y 2012 *J Mater Chem Phys* **134** 1172
[31] Yu A, Jiang P and Lin Wang Z 2012 *J Nano Energy* **1** 418
[32] Mohammed A A A, Suriani A B and Jabur A R 2018 *J Phys Conf Ser* **1003** 012070
[33] Dang Z M, Zheng M S and Zha J W 2016 *J Small* **12** 1688
[34] Mamat M H, Sahdan M Z, Khusaimi Z, Ahmed A Z, Abdullah S and Rusop M 2010 *J Opt Mater* **32** 696
[35] Liu X, Gu L, Zhang Q, Wu J, Long Y and Fan Z 2014 *J Nat Commun* **5** 1
[36] Vasudevan A, Jung S and Ji T 2011 *J ISRN Nanotechnol* **12** 2011
[37] Pawar R C, Shaikh J S, Suryavanshi S S and Patil P S 2012 *J Curr Appl Phys* **12** 778
[38] Manthina V, Pablo J, Baena C, Liu G and Agrios A G 2012 *J Phys Chemistry* **116** 23864
[39] Nafees M, Liaqut W, Ali S and Shafique M A 2013 *J Appl Nanosci* **3** 49